Sensors and Actuators B 178 (2013) 316–323

Contents lists available at SciVerse ScienceDirect

Sensors and Actuators B: Chemical

journal homepage: www.elsevier.com/locate/snb

Low-cost and portable refractive optoelectronic device for measuring wine fermentation kinetics

F. Jiménez-Márquez [a], J. Vázquez [a,*], J. Úbeda [b], J.L. Sánchez-Rojas [a]

[a] Microsystems, Actuators & Sensors Group, Escuela Técnica Superior de Ingenieros Industriales, Universidad de Castilla-La Mancha, Avenida Camilo José Cela, s/n, 13071, Ciudad Real, Spain
[b] Tecnología de los Alimentos, Universidad de Castilla-La Mancha, Avenida Camilo José Cela, s/n, 13071, Ciudad Real, Spain

ARTICLE INFO

Article history:
Received 26 September 2012
Received in revised form
20 December 2012
Accepted 24 December 2012
Available online 3 January 2013

Keywords:
Winemaking monitoring
Fermentation
Refractive index
Optoelectronics

ABSTRACT

The fermentation process that gradually turns must into wine influences to a large extent the characteristics of the final product. The quality of wines would largely benefit from exhaustive testing procedures during the whole fermentation. This work demonstrates the potential of refractive techniques to successfully record the fermentation kinetics by means of a low-cost and portable optoelectronic system, liable to be advanced into a fully automated prototype thanks to an observed trend change in refractive index. The system core features a laser diode and a PSD (position sensitive detector), achieving a sensitivity of 4.6×10^{-4} RIU (refractive index unit) on discrete samples, a similar figure to those reported by instruments utilized by enologists. The prototype has been validated with model solutions as a prior step toward the monitorization of the must fermentation in a laboratory fermenter. Consequently, it represents an alternative method to traditional areometry for recording the fermentation evolution.

1. Introduction

The key chemical compounds that define the evolution of the wine fermentation kinetics should ideally be reducing sugars, CO_2 production and ethanol. However, their measurement procedures are either expensive and complex [1,2] or time-consuming [3]. As the concentration of sugar and ethanol in a must sample is closely related to its density, which can be readily measured, wine makers rely in practice on the daily evolution of must density instead, until its full transformation into wine occurs. Due to the large number of factors that can influence the progress of a fermentation and that are in practice difficult to control (from the exact chemical content of the must supply, which varies in every fermentation, to the amount of dissolved oxygen during the process, among other factors), enologists rely on the rate of change of the density rather than on its absolute value at any given time during the progress of the fermentation. The changes undergone by the density during the fermentation are a result of yeast metabolism. Specifically, the gradual depletion of glucose and fructose leads to the formation of ethanol, glycerol and carbon dioxide as major by-products, along with biomass [4,5].

The must fermentation evolution is typically overseen by enologists, who are in charge of the manual extraction and subsequent analysis of discrete samples. This routine proceeds at least once a day and usually for fifteen days or more. A correct fermentation process is a necessary condition but not sufficient by itself to determine the final quality of the wine, whose assessment relies on a comprehensive analysis of its chemical components, as the basic flavor of wine depends on at least 20 compounds [4].

Currently, in big cellars typical in La Mancha region (Spain), where production rates are massive, density is traditionally analyzed using areometers, instruments based on the Archimedes' principle [3] with an optimal sensitivity of 0.5 g/L. Although commercially available, high-accuracy instruments based on an U-shaped resonator report a remarkable sensitivity figure of 0.005 g/L, they are expensive and ultimately do not prevent enologists from the daily sample extraction and subsequent analysis.

Aiming at improving the wine quality and thereby sink its production costs, a number of schemes have been tested over the past years in order to automatically supervise the fermentation kinetics in real time. These schemes are: (1) density monitoring based on differential pressure measurements [6,7]; (2) carbon dioxide monitoring [6–8]; (3) determination of yeast cells population evolution using both impedance techniques [9] and turbidity measurements [10]; (4) ultrasound measurements conducted to determine the propagation velocity in must [11]; (5) optical fiber refractometry [12,13]. None of these schemes have proved totally satisfactory: either the technique simply lacks sufficient accuracy, or measurements were performed solely on discrete samples, or the sensor reading performance deteriorates dramatically due to an

* Corresponding author. Tel.: +34 926295300x3899.
E-mail address: javier.vazquez@uclm.es (J. Vázquez).

0925-4005/$ – see front matter © 2013 Elsevier B.V. All rights reserved.
http://dx.doi.org/10.1016/j.snb.2012.12.091

increasing deposition of tartaric acid crystals on the sensor active surface [13].

The use of refractometric techniques has become widespread in a number of fields due to its accuracy, reduced size, response velocity and immunity to electromagnetic interference. Some commercial refractometers are based on the measurement of the critical angle. Their sensitivity may vary from 1×10^{-3} in hand-held refractometers or 1×10^{-4} in some Abbé refractometers to 1×10^{-6} in some sophisticated digital refractometers. In addition to this, a number of refractometric measurement procedures rely on the use of optical fibers as they are characterized by a large sensitivity, depending their specific figures of merit on their underlying operating principle [14]. To mention some of them, the reported sensitivity of optical fiber systems based on Bragg gratings is 7.2×10^{-6} RIU; sensor systems relying on the total internal reflection phenomenon have a sensitivity of up to 1.5×10^{-4} RIU in measurements carried out in concentrated solutions [15]; multimodal interference methods reach a sensitivity value of 4.6×10^{-6} RIU [14], whereas some schemes utilize a PSD as a beam detector and its performance is thus strongly determined by the total length of the optical path. Reported sensitivities are 4×10^{-7} RIU [16] and 0.012% (equivalent to 1.2×10^{-5} RIU, upon conversion) in instruments devised for salinity measurements [17]. There exist also critical-angle refractometers featuring a photodiode array as the beam detector reporting a sensitivity of 5×10^{-4} RIU [18].

This paper demonstrates that not only is refractometry a suitable alternative technique to record the evolution of grape must fermentation, but it also gives a competitive edge over the standard technique based on density since it allows to determine the end of the fermentation in a novel way that, besides, is liable to be automated and thus detected without the aid of external supervision. Refractometry measurements were made with an optoelectronic prototype reaching a sensitivity of 4.6×10^{-4} RIU. Although there exist a number of techniques to achieve a finer sensitivity, the developed system has a number of additional advantages: it is a portable and independent module, its overall cost is kept reasonably low (approximately one order of magnitude less than commercially available hand-held refractometers and two orders of magnitude less than desk Abbé refractometers) as it does not require any expensive components, and it was designed to avoid physical contact with the fluid samples, which grants a high degree of robustness and keeps maintenance works to a minimum (tartaric acid crystals would never deposit on the sensor active surface with the proposed scheme, although a cleaning procedure could eventually be advisable in a further development of the prototype). Moreover, it should be stressed the fact that fermenting must is a rather inhomogeneous fluid of turbid nature, containing a large amount of suspended particles in motion that come in a variety of sizes. Its inhomogeneous nature do not let benefit from measuring with the highest sensitivity available, as deviations in consecutive measurements are expected to be relatively large. Consequently, not single but average measurements instead are representative of the actual refractive index value, for which the highest accuracy is not essential.

2. Material and methods

2.1. Model solutions

Both model solutions and natural grape musts were utilized in the experiments. Model solutions proved useful at an initial stage to test the performance of the measurement system and eventually validate it. Two different sets of model solutions were prepared, both of them containing nine solutions. Each solution is a particular mixture of glucose (from 100 to 1 g/L), fructose (from 110 to 2 g/L), ethanol (from 0% to 14% v/v) and glycerol (from 0 to 8 g/L) dissolved in water. The first set represents a normal fermentation, that is, both density and concentrations of major metabolic compounds match those of an ordinary fermentation. The second set represents a stopped or sluggish fermentation, characterized by density and concentration change rates close to zero once half fermentation has been reached. A variety of reasons may be attributable to this kind of unnormal fermentations, which occasionally occur. Among them are the lack of dissolved oxygen, an unbalanced ratio between sugar and assimilable nitrogen in grape must, low fermentation temperature, inadequate rehydration or thermal shock of yeast, etc.

Tables 1 and 2 show the compositions of all 9 prepared solutions belonging to the normal and to the sluggish set, respectively.

2.2. Winemaking

Cencibel variety first press red grape must from the 2011 vintage was supplied by "El Progreso" cellar located in La Mancha region. It was kept frozen at −20 °C and slowly defrosted prior to use in a refrigerated chamber, including vigorous shakes carried out at periodic intervals in order to homogenize the fluid.

Four fermentations were completed using 10% (w/v) of red grape skin added to *Cencibel* must according to the proportion utilized in the wine cellar. The must was inoculated with 10^6 cells/mL of *Saccharomyces cerevisiae* strain (UCLM S325, Fermentis) previously rehydrated following the supplier's guidelines. A 5 L-cylindrical fermenter, featuring a length-diameter ratio similar to that of an industrial one, was filled with 4 L of inoculated must and grape skins.

The laboratory fermenter was plunged in a temperature-controlled water bath at 26 °C. A customized squeezer was used to immerse the skins deep into the must.

The fermentation monitoring was carried out by means of the extraction and analysis of 10 mL-samples every 12 h approximately during 7 days. The tubular fermenters were stirred with their respective squeezers prior to the extraction of samples. On the other hand, standard aerometry was used for density measurements inside the fermenters.

After extraction samples were centrifuged for ten minutes at 4500 rpm, filtered using a pore size of 0.45 μm and kept refrigerated until analysis. Glucose, fructose, glycerol and ethanol were analyzed by a high-performance liquid chromatography (HPLC) system (Jasco, Japan) equipped with a refractive index detector. Chromatographic separation was performed in a BioRad HPX-87H (300 mm × 7.8 mm) column thermostatised at 25 °C. Sulphuric acid (0.245 g/L) was used as the mobile phase; flow rate was 0.5 mL/min.

The assessment of the fermentation stage was carried out for each sample measuring with the optoelectronic prototype and, as stated previously, a sensitivity of 4.6×10^{-4} RIU was achieved. Each sample was measured three times; the resulting deviations arise from the minor variations in the positioning of the cuvette inside its cavity every time. Refractive index values were obtained at 20 °C over a short period of time in a thermostatised lab, being the maximum variation of temperature during the process below ±0.5 °C. An estimate of the change in refractive index arising from this deviation in temperature, based on data for fresh musts [3], is $\pm 8.5 \times 10^{-5}$ RIU. This figure is one order of magnitude lower than the resolution of our system.

In an industrial fermentation process temperature fluctuations would influence to some extent the refractive index measurements. Therefore it would be useful to implement corrections in the software, depending on the temperature and the major components of the sample under test. In a similar fashion, density tables are widely utilized to date by enologists in order to determine the density at 20 °C during the whole fermentation. Nevertheless, it is the

Table 1
Glucose, fructose, total sugar, ethanol and glycerol concentrations of all nine solutions belonging to the normal set.

Solution	Glucose (g/L)	Fructose (g/L)	Total sugar (g/L)	Ethanol (% v/v)	Glicerol (g/L)
1	100	110	210	0	0
2	80	90	170	1	0
3	30	70	100	6	5
4	20	60	80	8	5
5	10	40	50	9	6
6	2	20	22	12	7
7	2	8	10	13	7
8	2	5	7	13	7
9	1	2	3	14	8

Table 2
Glucose, fructose, total sugar, ethanol and glycerol concentrations of all nine solutions belonging to the sluggish set.

Solution	Glucose (g/L)	Fructose (g/L)	Total sugar (g/L)	Ethanol (% v/v)	Glicerol (g/L)
1	100	110	210	0	0
2	80	90	170	1	0
3	60	80	140	3	3
4	30	70	100	6	5
5	27	66	93	7	5
6	26	64	90	7	5
7	24	62	86	7	6
8	22	58	80	7	6
9	21	57	78	8	7

variations (either of density or refractive index in our case) that help enologists determine the current fermentation status, and whether or not corrective measures are required as it progresses.

In the case of fresh musts prior to fermentation the obtained sensitivity was 1.2 g/L. Additional instruments were utilized in the whole set of measurements involved in every fermentation. A hand-held ocular refractometer (Milwaukee MR330ATC) with a sensitivity of 8×10^{-4} RIU was utilized to check deviations with the measurements performed by the prototype.

2.3. System design

The prototype as a whole comprises two major elements. On one hand, a polyamide frame properly mechanized holds tightly both the optoelectronic elements and the must sample. Fig. 1 is a diagram illustrating the relative location of the laser diode, the PSD and the must sample in between. The laser diode peaks at 655 nm (ADL-65055TL by Laser Components) and is inserted inside a collimator (LT110P-B by Thorlabs), whereas the PSD has an active area of $1 \times 6\,mm^2$ (S3931 by Hamamatsu). The temperature sensor (LM35 by National Semiconductor) is a silicon integrated sensor that can be immersed in the must sample (not shown). On the other hand, a customized printed circuit board was designed to polarize the optoelectronic devices and perform the signal conditioning as well. At this stage of the development two additional test elements complete the system: a data acquisition board USB-6211 by National Instruments, which samples the voltage signals and performs the analog-to-digital conversion, and a laptop utilized for the signal processing and the display of key data by means of a virtual instrument programmed with Labview software. In a further stage it is foreseeable that both the data acquisition board and the laptop will be replaced with a small microcontroller-based board.

2.3.1. Mechanical structure

Fig. 2 shows a photograph of the supporting frame. All the necessary geometrical features were engineered with SolidWorks and

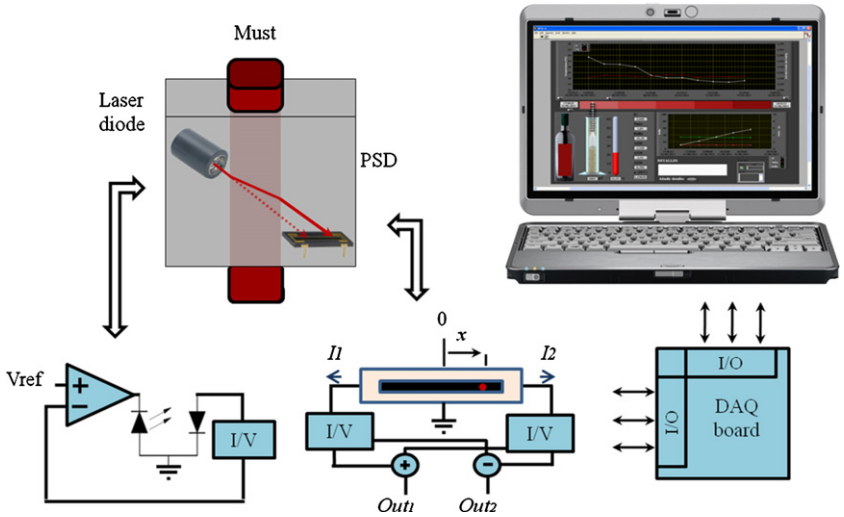

Fig. 1. Operating principle and prototype overview: mechanical structure, optoelectronic schemes, conditioning circuits, data acquisition and display. x represents the spot position; I_1 and I_2 are the photocurrents delivered at both PSD electrodes; Out_1 and Out_2 are, respectively, addition and subtraction of the two photocurrent signals after conversion to voltages.

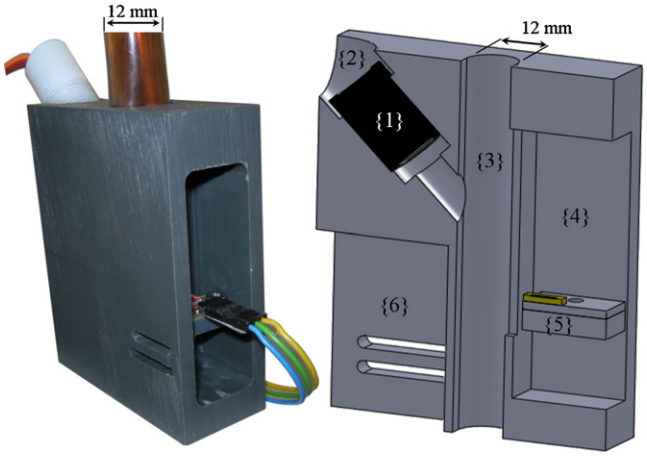

Fig. 2. Prototype's mechanical structure: real view and section view showing all its features and the placement of the optoelectronic devices in relation to the must samples. It comprises the following parts: {1} laser diode and collimator; {2} fastener that locks the laser diode inside its cavity; {3} cavity to lodge the sample; {4} cavity to allocate the PSD at its corresponding height; {5} PSD and corresponding PSD holder; {6} cavity to allocate the conditioning electronics.

mechanized on a polyamide block. The structure was designed to hold the laser diode, the PSD and the sample in an optimal configuration that allows the measurement of the refractive index n while avoiding misalignments and vibration coupling. The sample cavity was devised to be used both with spectrophotometer cuvettes (featuring a 10 mm-optical path) and flexible tube properly shaped in order to accomplish parallel plane sides to be traversed by the laser beam. Although the deposition of tartaric acid crystals and microbial biomass is not an issue at this stage (only filtered samples are measured in this work), the proposed scheme would keep the crystals from depositing on the active surface of the sensors if unfiltered samples were utilized. Such depositions would still occur on the walls of the tube containing the fluid and might eventually compromise the optical path; therefore, it is foreseeable that a further development of the prototype might include a cleaning procedure of the tube. Alternatively, other options will be considered where measurements may be carried out without the need of a tube or a cuvette in the optical path.

2.3.2. Electronic schemes

Fig. 1 shows some diagrams representing the electronic stages utilized for the laser diode excitation and the PSD signal conditioning. The laser diode stage delivers a stable power output by means of an integrated photodiode and a transimpedance amplifier, being both elements part of a feedback loop. The PSD signal conditioning is performed with two transimpedance amplifiers, one for each of the generated photocurrents that are combined using a summing and a difference amplifier. This differential approach allows to know the accurate position of the laser spot on the PSD active area. A detailed description of the electronic modules is out of the scope of this work.

3. Theory

3.1. Theoretical fundamentals

One of the most common procedures for assessing the density, the sugar content and the probable alcohol content to be obtained from fresh musts before fermentation takes place is based on refractometry [3]. It has become a very popular method since it yields results fast and besides tiny amounts of sample are needed. We recall at this point that both the density and the sugar content of musts can be derived from refractometric measurements thanks to cross-referenced data published in standardized tables for several temperatures. A proportionality relationship holds between the glucose and fructose concentration, on one hand, and refractive index and density, on the other hand [19,20]. That is, the larger the sugar concentration, the larger the density and the refractive index. Changes in the relative concentrations of fructose and glucose do not alter significantly the proportionality constants as both sugars are very similar [19] and thus fresh musts can be regarded as binary mixtures composed solely of water and sugar.

However, refractometry is not considered by the International Organization of Vine and Wine as a measurement procedure once the fermentation process has begun. The technique has been disregarded as the proportionality relations between refractive index and density, on one hand, or refractive index and total sugar content, on the other hand, no longer hold after the fermentation process has set off, simply because must can only be considered a binary mixture before alcohol formation takes place. The transformation of glucose and fructose into ethanol and glycerol as by-products of the fermentation reaction influences density and refractive index in different ways. The gradual depletion of fructose and glucose implies a reduction in both density and refractive index values. The ratio between glucose and fructose concentrations plays a minor role in the observed decreasing trend of the two parameters [21]. As for glycerol, its formation contributes to increase both parameters, whereas an increase in ethanol concentration has opposite effects on density and refractive index: density undergoes a decrease but refractive index an increase [19,20,22]. As a consequence of these observations it can be concluded that the aforementioned proportionality relation breaks once the fermentation reaction has been triggered and alcohol starts to form.

Even though there exists no linear relationship between density and refractive index (after all, they are two different physical parameters and such linearity should not be expected at all), it does not prevent the refractive index from being a suitable indicator to successfully gauge the fermentation kinetics, in the same way as density does. According to data obtained from mixtures containing fructose, glucose and ethanol dissolved in water, refractive index is proportional to the concentration of all three compounds. The largest increase occurs in the cases of glucose and fructose as the refractive index of ethanol is the closest to that of water and thus ethanol has the least influence on the refractive index of the mixture [22]. It has also been observed that, for a given ethanol concentration, the increase in the fructose and glucose concentrations influences the refractive index in a way that is independent of the fixed concentration of ethanol [21,22].

3.2. Operating principle

The sensing principle of the refractive index is based on Snell's law. A laser beam generated in a laser diode hits a surface with a certain angle of incidence and passes through a must sample of known width making a different angle with the normal to the surface. The beam undergoes then a second change in direction, leaving the sample parallel to the incident beam and finally reaching the PSD active surface. The PSD outputs two current signals that combined represent an accurate measure of the laser spot position on its surface.

The underlying principle the refractive index measurements are based on is illustrated in Fig. 3. According to Snell's law, when the properties of the must change as the concentrations of glucose, fructose, ethanol and glycerol vary, the trajectory of the laser beam shifts gradually until the fermentation reaction is finished. This progress is tracked by the PSD in a discrete fashion, sample by sample. Notice that water is considered too, as water is necessary at the calibration stage. Since $n_w < n_m$, it follows that $\theta_w > \theta_m$.

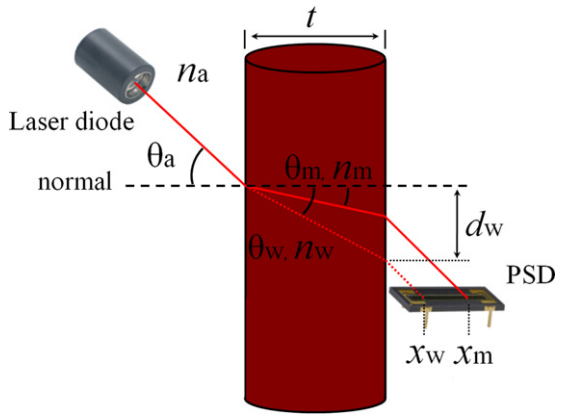

Fig. 3. Operating principle of the refractive index technique. The variables are as follows. n_a: refractive index in air; n_w: refractive index in water; n_m: refractive index in must; θ_a: angle of incidence at the air-liquid interface; θ_w: refractive angle in water; θ_m: refractive angle in must; t: sample thickness; x_w: reference position on the PSD surface when the sample is water; x_m: spot position on the PSD of a given must sample; d_w: beam shift from the normal on the back surface of the cell when the sample is water.

The refractive index n_m of a given must sample can be figured out using (1) provided the position of the laser beam on the PSD active surface x_m is known. An inspection of expression (1) shows that the refractive index is a function of the angle of incidence θ_a, the sample thickness t, and the shift $x_m - x_w$ undergone by the beam, taking water as the necessary reference.

$$n_m = \frac{n_a \times \sin(\theta_a)}{\sin\left(\tan^{-1}\left(d_w - \left[|x_m - x_w| \times \tan(\theta_a)\right]/t\right)\right)} \quad (1)$$

As stated previously, refractometry is a technique that has been deployed in a number of different applications so far, from pioneering schemes [23,24] to more sophisticated set ups devised to measure the salinity of certain solutions [16,17]. Further interesting approaches closely related to this work are the measurement of concentrations of binary mixtures formed by ethanol dissolved in water [20], and the measurement of refractive index of wine, considered as a finished product [25,26].

4. Results and discussion

4.1. Model solutions

Density and refractive index of the model solutions were measured for normal and sluggish fermentations using a standard areometer and the optoelectronic prototype, respectively.

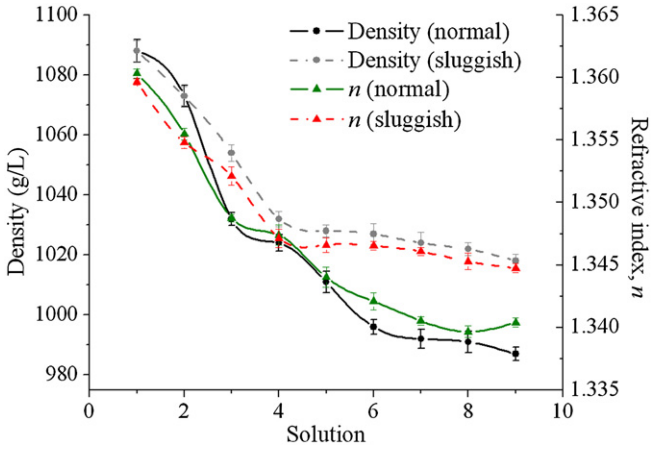

Fig. 4. Refractive index n versus density for both the normal and the sluggish sample sets.

Experiments performed using the normal set of solutions previously defined reproduce a density curve that resembles that of an ordinary must fermentation (Fig. 4). As can be seen, density decreases swiftly with the sample number from the beginning but ends up leveling out in the last three or four samples. However, when changing to the sluggish set the scenario is a completely different one since density stabilizes as of the fourth sample due to an abrupt stop. These results are in agreement with the sugar and alcohol concentration data shown in Tables 1 and 2: a change in the sugar content, regardless of its magnitude, translates into a similar change in density.

As for the refractive index, its trend does not match exactly the one observed for the density for the reasons outlined in section 3.1 Theoretical fundamentals. Nevertheless, the same conclusions can be derived. Observe the slight increase registered with the normal set toward the end of the fermentation. This peculiarity is not a distinctive feature of the model solutions under test since it arises in actual fermentations too, as will be detailed next. These results complete satisfactorily the validation of the optoelectronic system utilized in the measurements of both sets of solutions and thus it can be utilized to measure fermenting must samples.

4.2. Winemaking

Having checked the theoretical background for using the refractive index as a valid gauge of the fermentation kinetics and subsequently verified and validate the performance of the

Table 3
Glucose, fructose, total sugar, ethanol and glycerol concentrations for fermentation a (Fig. 5) by HPLC. σ is the standard deviation.

Time (hours)	Glucose (g/L)	σ	Fructose (g/L)	σ	Total sugar (g/L)	Ethanol (% v/v)	σ	Glycerol (g/L)	σ
0.0	101.3	0.7	104.7	0.7	206.0	0.0	0.0	0.0	0.0
9.7	102.3	0.1	106.1	0.1	208.4	0.0	0.0	0.0	0.0
22.8	84.4	0.1	90.3	0.0	174.7	0.0	0.0	0.0	0.0
33.4	73.7	0.1	88.6	0.1	162.4	1.3	0.0	1.1	0.0
46.7	47.2	0.1	79.0	0.2	126.2	4.6	0.0	4.0	0.0
58.2	28.7	0.4	63.9	0.9	92.6	5.7	0.2	4.6	0.1
70.4	17.8	0.1	54.7	0.1	72.5	7.0	0.1	5.2	0.0
81.9	9.3	0.0	44.0	0.0	53.3	8.2	0.1	2.8	3.9
97.5	2.8	0.0	29.8	0.1	32.6	10.5	0.1	6.6	0.0
105.2	1.9	0.2	21.5	0.3	23.4	10.9	0.0	6.9	0.0
119.3	1.1	0.1	7.9	0.0	9.0	10.0	0.5	6.9	0.2
130.7	1.4	0.1	4.7	0.2	6.1	11.1	0.0	7.1	0.0
143.7	1.8	0.0	3.0	0.0	4.8	11.1	0.1	7.2	0.0
153.3	1.7	0.1	2.6	0.1	4.3	11.7	0.2	7.4	0.2
167.9	2.0	0.0	2.1	0.1	4.1	11.1	0.3	7.6	0.3
172.5	1.8	0.0	2.2	0.0	3.9	11.7	0.2	7.9	0.0

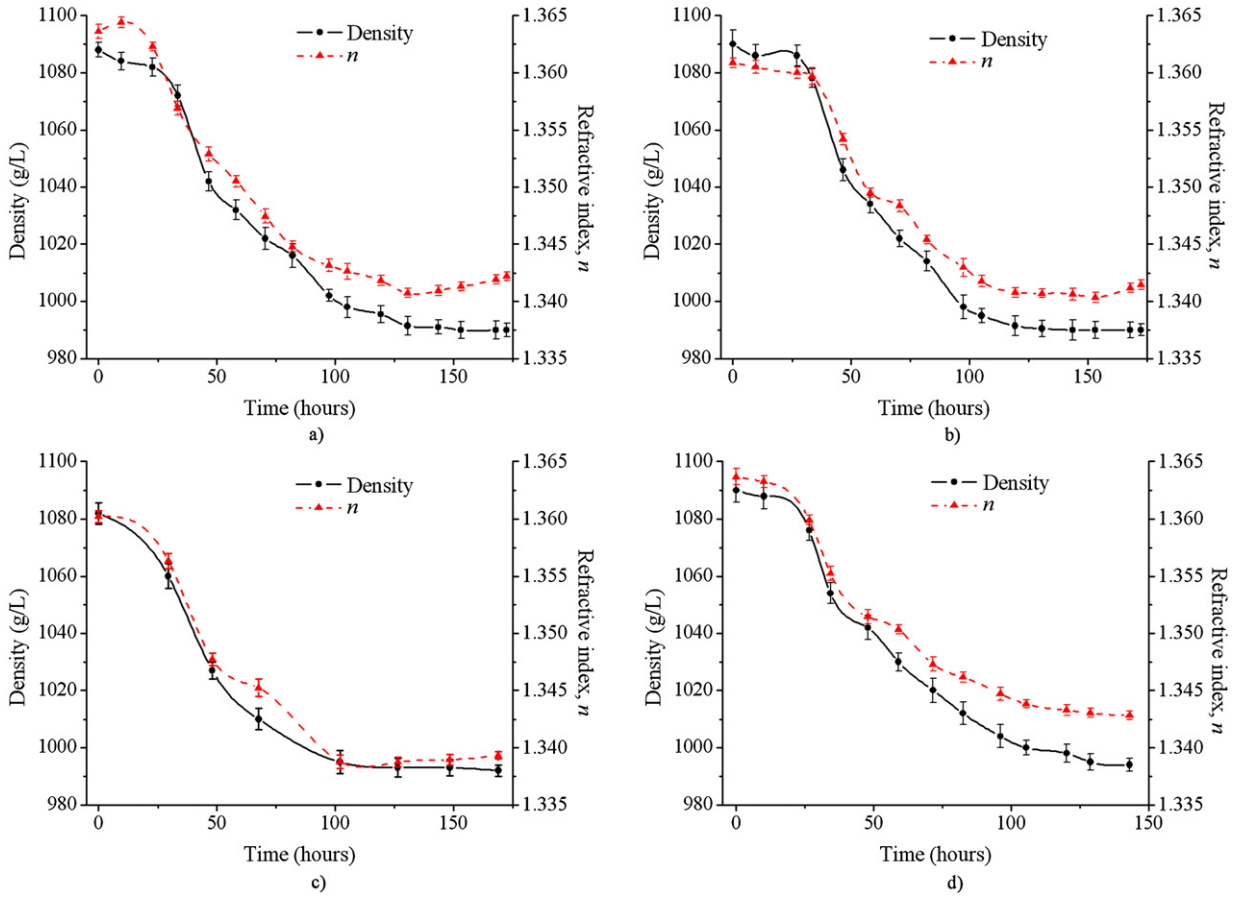

Fig. 5. Refractive index *n* versus density evolution in winemaking. (a–c) Represent finished fermentations whereas figure d represents an unfinished one.

Table 4
Glucose, fructose, total sugar, ethanol and glycerol concentrations for fermentation b (Fig. 5) by HPLC. σ is the standard deviation.

Time (hours)	Glucose (g/L)	σ	Fructose (g/L)	σ	Total sugar (g/L)	Ethanol (% v/v)	σ	Glycerol (g/L)	σ
0.0	106.6	0.0	109.1	0.0	215.7	0.0	0.0	0.0	0.0
9.7	104.8	0.0	108.0	0.0	212.9	0.0	0.0	0.0	0.0
27.2	93.6	0.2	98.7	0.3	192.2	0.1	0.0	0.0	0.0
33.4	78.0	0.1	90.6	0.1	168.6	1.0	0.0	0.8	0.0
46.7	50.9	0.4	81.0	0.6	131.9	4.9	0.0	3.8	0.0
58.2	32.0	0.2	69.0	0.4	101.0	6.7	0.0	4.8	0.0
70.4	19.8	0.4	60.1	1.0	79.9	8.7	0.1	5.7	0.1
81.9	9.1	0.1	43.1	0.5	52.2	9.4	0.2	5.7	0.1
97.5	3.5	0.1	28.5	0.6	32.0	12.2	0.1	7.2	0.2
105.2	2.5	0.2	19.4	0.2	21.9	12.9	0.0	7.4	0.1
119.3	2.2	0.0	8.7	0.0	10.9	13.0	0.0	7.4	0.0
130.7	1.5	0.0	4.9	0.1	6.4	13.1	0.3	7.4	0.1
143.7	1.9	0.0	2.9	0.0	4.8	13.1	0.1	7.5	0.0
153.3	2.0	0.1	2.2	0.1	4.2	13.2	0.4	7.8	0.2
167.9	2.2	0.0	1.6	0.0	3.8	13.2	0.1	7.8	0.0
172.5	1.8	0.1	1.4	0.0	3.2	13.4	0.4	7.8	0.2

Table 5
Glucose, fructose, total sugar, ethanol and glycerol concentrations for fermentation c (Fig. 5) by HPLC. σ is the standard deviation.

Time (hours)	Glucose (g/L)	σ	Fructose (g/L)	σ	Total sugar (g/L)	Ethanol (% v/v)	σ	Glycerol (g/L)	σ
0.0	100.0	0.3	100.0	0.3	199.9	0.0	0.0	0.0	0.0
29.5	62.0	0.6	83.0	0.8	145.0	0.0	0.0	2.5	0.0
48.0	28.4	0.5	66.2	1.1	94.7	2.9	0.1	5.6	0.1
67.5	10.7	0.2	39.2	0.4	49.9	7.8	0.1	5.9	0.1
102.0	1.5	0.0	4.3	0.0	5.9	10.5	0.0	6.8	6.8
126.5	1.9	0.0	1.5	0.0	3.4	11.0	0.1	6.8	0.0
148.5	2.3	0.0	1.3	0.0	3.6	10.8	0.0	6.9	0.0
169.0	1.8	0.3	0.9	0.1	2.7	11.1	0.2	6.9	0.7

Table 6
Glucose, fructose, total sugar, ethanol and glycerol concentrations for fermentation d (Fig. 5) by HPLC. σ is the standard deviation.

Time (hours)	Glucose (g/L)	σ	Fructose (g/L)	σ	Total sugar (g/L)	Ethanol (% v/v)	σ	Glicerol (g/L)	σ
0.0	107.4	0.1	107.5	0.1	214.9	0.0	0.0	0.0	0.0
10.0	107.1	0.1	107.0	0.1	214.1	0.0	0.0	0.0	0.0
26.5	81.7	0.3	98.0	0.3	179.7	0.0	0.0	1.9	0.0
34.3	58.8	0.0	86.1	0.0	144.9	1.2	0.0	3.7	0.0
47.8	38.4	0.1	75.1	0.3	113.5	3.4	0.0	5.4	0.0
59.0	26.5	0.1	64.8	0.1	91.3	4.5	0.0	5.9	0.0
71.5	17.8	0.0	48.0	0.1	65.8	7.6	0.0	5.9	0.1
82.5	11.6	0.1	37.6	0.4	49.2	8.1	0.2	6.3	0.1
96.0	7.6	0.1	29.4	0.5	37.0	8.4	0.1	6.4	0.1
105.5	5.8	0.0	24.7	0.1	30.5	8.6	0.1	6.8	0.1
120.2	3.7	0.0	18.4	0.0	22.1	8.8	0.0	6.6	0.1
128.8	2.9	0.1	15.2	0.3	18.1	9.2	0.1	6.7	0.2
143.0	2.2	0.1	12.7	0.7	14.9	9.6	0.4	7.3	0.6

measurement prototype with model solutions, a number of red wine fermentations were carried out and monitored.

Fig. 5 represents the evolution in terms of density and refractive index of four different red wine fermentations, measured in the same way as in the previous section. Both density and refractive index follow a rather similar trend, as observed previously with the model solutions.

The major difference emerges once again when density values start to stabilize near the end of the process: as can be seen, the density levels out around a value of 990 g/L, whereas the refractive index undergoes a little but distinctive increase around 130 hours after the fermentation started (Fig. 5 a, b and c). At this late stage the sugar content was always less than 5 g/L, as can be seen in Tables 3–5 for fermentations a, b and c. Specifically, the residual sugar content was 4.8 g/L, 3.8 g/L and 3.4 g/L for these three fermentations, respectively. This phenomenon, that has been observed repeatedly both with the optoelectronic prototype and a hand-held ocular refractometer, opens a door to a fully automation of the fermentation supervision, as the trend change can readily be detected by an algorithm implemented in software and is in all cases very close to the 2–3 g/L accepted as the standard interval the fermentation end falls within [27,28].

In order to stress the potential of the trend change observed in the refractive index to determine the end of the fermentation, a final remark will be added concerning the fermentation corresponding to Fig. 5d. As can be seen, both density and refractive index follow similar trends as expected. As the density started to level out at a value of 994 g/L after 143 hours, the process was regarded as finished according to the ordinary criterion that tracks the density evolution. However, upon sample analysis via HPLC it was noticed that there were still 14.9 g/L of remaining sugar, as can be seen in Table 6, which leads to think that the fermentation had not come to a complete stop yet. This is in agreement with the absence of trend change in the refractive index curve. Had the novel criterion proposed in this work been observed, the fermentation would have gone on for some more time.

5. Conclusions

In order to contribute to the automation of fermentations at large scale an optoelectronic prototype has been developed. Even though refractive index and density behave in a slightly different way during the fermentation of must, it has been demonstrated that the kinetics associated to an ordinary fermentation process can be satisfactorily followed by registering the evolution of the refractive index of the grape must fermentation instead of its density, parameter traditionally recorded in wine cellars. This procedure allows the enologist to follow the progress of a fermentation in terms of the rate of change of the refractive index. A remarkable feature of the proposed method is its potential to automatically detect when the fermentation has come to its end in an easy and reproducible way (specifically, when the residual sugar content is less than 5 g/L, very close to the 2–3 g/L ideally expected). This is of particular interest in very big cellars with massive production of several million liters, where fermentations last for at least 15 days.

The operating principle of the prototype relies on refractometry and is a robust, inexpensive and portable system. At the current stage the prototype has reached a sensitivity of 4.6×10^{-4} RIU for measuring refractive index and 1.2 g/L for measuring density in must (before the fermentation begins). It is versatile enough to be advanced into a fully automated phase where readings would be processed in real time with the aid of an additional hydraulic system, engineered to continuously pump must into the system during the whole fermentation span.

Acknowledgement

This work has been supported by MICINN (Spain) under project contract DPI2012-31203. The authors wish to thank Francisco Jiménez Navas and Pedro Jiménez de los Galanes for the mechanization of the mechanical models used in this work; Juan Nieto, enologist at "El Progreso" wine cellar (Villarrubia de los Ojos, Spain) for facilitating the must, and María Chacón for her work with the HPLC system.

References

[1] V. Bellon, Fermentation control using ATR and an FT-IR spectrometer, Sensors Actuators B: Chemical 12 (1993) 57–64.
[2] R. Vonach, B. Lendl, R. Kellner, High-performance liquid chromatography with real-time Fourier-transform infrared detection for the determination of carbohydrates, alcohols and organic acids in wines, Journal of Chromatography A 824 (1998) 159–167.
[3] OIV, Compendium of International Methods of Wine and Must Analysis, International Organisation of Vine and Wine, Paris, 2011.
[4] R.S. Jackson, Wine Science, Principles and Applications, third ed., Acedemic Press, London, 2008.
[5] R.B. Boulton, V.L. Singleton, L.F. Bisson, R.E. Kunkee, Principles and Practices of Winemaking, Chapman & Hall, New York, 1996.
[6] N. El Haloui, D. Picque, G. Corrieu, Alcoholic fermentation in winemaking: on-line measurement of density and carbon dioxide evolution, Journal of Food Engineering 8 (1988) 17–30.
[7] E.T. Nerantzis, P. Tartaridis, I.A. Sianoudis, X. Ziani, E. Tegou, Winemaking process engineering: on line fermentation monitoring - sensors and equipment, E-Journal for Science and Technology 2 (2007) 29–36.
[8] S. Wieland, Verfahren zum kontrollierten Vergären einer Flüssigkeit, European Patent (2006) EP 1 559 775 A3.
[9] M.A. Pérez, R. Muñiz, C. de la Torre, B. García, C.E. Carleos, R. Crespo, L.M. Cárcel, Impedance spectrometry for monitoring alcoholic fermentation kinetics under wine-making industrial conditions, in: XIX IMEKO World Congress Fundamental and Applied Metrology, Lisbon, Portugal, 2009, pp. 2574–2578.
[10] R. Crespo, L.M. Cárcel, M.A. Pérez, I. Nevares, M. del Álamo, Suitable at-line turbidity sensor for wine fermentation supervision, in: International Conference for Food Innovation, Valencia, Spain, 2010, pp. 1–4.
[11] N. Lamberti, L. Ardia, D. Albanese, M. Di Matteo, An ultrasound technique for monitoring the alcoholic wine fermentation, Ultrasonics 49 (2009) 94–97.

[12] Cao y PazF A.M., J.M. Acevedo, J. Doval, A. del Río, C. Martínez-Peñalver, M.L. Soria, Plastic optical fiber sensor for real time density measurements in wine fermentation, in: Instrumentation Measurement and Technology Conference – IMTC 2007, Warsaw, Poland, 2007, pp. 1–5.
[13] C. Quintáns, J.M. Acevedo, A.M. Cao, M.J. Paz, Graña, Experiences in measuring density by fiber optic sensors in the grape juice fermentation process, in: XIX IMEKO World Congress Fundamental and Applied Metrology, Lisbon, Portugal, 2009, pp. 2579–2582.
[14] R.X. Gao, W.J. Liu, Y.Y. Wang, Q. Wang, F. Zhao, S.L. Qu, Design and fabrication of SMS fiber refractometer for liquid, Sensors Actuators A: Physical 179 (2012) 5–9.
[15] I. Noiseux, W. Long, A. Cournoyer, M. Vernon, Simple fiber-optic-based sensors for process monitoring: An application in wine quality control monitoring, Society for Applied Spectroscopy 58 (2004) 1010–1019.
[16] D. Malardé, Z.Y. Wu, P. Grosso, J.-L. de Bougrenet, M. Le Menn, High-resolution and compact refractometer for salinity measurements, Measurement Science and Technology 20 (2009) 015204 (8 pp.).
[17] Y. Zhao, B. Zhang, Y. Liao, Experimental research and analysis of salinity measurement based on optical techniques, Sensors Actuators B: Chemical 92 (2003) 331–336.
[18] J.E. Geake, C.S. Mill, The Cassini-Huygens SSP refractometer: REF, Planetary and Space Science 46 (1998) 1409–1414.
[19] D.R. Lide, CRC Handbook of Chemistry and Physics, eighty-fifth ed., Internet Version 2005, http://www.hbcpnetbase.com. CRC Press, Boca Raton, FL, 2005.
[20] Y.-L. Yeh, C.C. Wang, M.-J. Jang, Y.-P. Lin, A high-precision measurement technique for evaluating alcohol concentrations using an optical metrology system based on a position sensing detector, Optics and Lasers in Engineering 47 (2009) 599–603.
[21] A.E. Flood, S. Puagsa, Refractive index, viscosity, and solubility at 30 °C, and density at 25 °C for the system fructose + glucose + ethanol + water, Journal of Chemical and Engineering Data 45 (2000) 902–907.
[22] A.E. Flood, J. Addai-Mensah, M.R. Johns, E.T. White, Refractive index, viscosity, density, and solubility in the system fructose + ethanol + water at 30, 40, and 50 °C, Journal of Chemical and Engineering Data 41 (1996) 418–421.
[23] S. Nemoto, Measurement of the refractive index of liquid using laser beam displacement, Applied Optics 31 (1992) 6690–6694.
[24] F. Docchio, S. Corini, M. Perini, R.S. Kasana, A simple and reliable system for measuring the refractive index of liquids using a position-sensitive detector, IEEE Transaction on Instrumentations and Measurement 4 (1995) 68–70.
[25] J. Mutanen, J. Räty, E. Gornov, P. Lehtonen, K.-E. Peiponen, T. Jaaskelainen, Measurement of color, refractive index, and turbidity of red wines, American Journal of Enology and Viticulture 58 (2007) 387–392.
[26] I. Niskanen, J. Mutanen, P. Lehtonen, J. Räty, M. Yamaguchi, K.-E. Peiponen, T. Jaaskelainen, Multifunction spectrometer for optical inspection of red wine, Sensing and Instrumentation for Food Quality and Safety 2 2 (2008) 58–65.
[27] P. Ribéreu-Gayon, D. Dubourdieu, B. Donèche, A. Lonvaud, Handbook of Enology The Microbiology of Wine and Vinifications, vol. 1, second ed., John Wiley & Sons, Chichester, 2006.
[28] J. Hidalgo, Tratado de Enología, Tomo 1, segunda ed, Mundi-Prensa, Madrid, 2011.

Biographies

Francisco Jiménez Márquez received his M.Sc. degree in industrial engineering from the Universidad de Castilla–La Mancha (Spain) in 2010, and a post-graduate master's degree in micro/nanoelectronics from Universidad de Sevilla (Spain) in 2011. He is currently working toward the Ph.D. degree with the Microsystems, Actuators and Sensors group from the Universidad de Castilla–La Mancha, Ciudad Real (Spain). His research interests are in optoelectronic sensors and systems for food quality monitoring.

Javier Vázquez del Real received his M.Sc. degree in physics from the Universidad de Valencia (Spain) in 1992 and the Ph.D. degree from the Universidad de Castilla–La Mancha (Spain) in 2006. He worked for a year at the Valencian Institute for Agricultural Research (Spain). He has previous working experience in the industry in corporations like Alcatel, Bosch and Valeo (Germany and Spain). He was a guest member of staff at Newcastle University (UK) during a postdoctoral stay in 2007 and 2008. Currently he is a lecturer at the Universidad de Castilla–La Mancha.

Juan Úbeda Iranzo graduated in Pharmacy (Universidad de Valencia), is Ph.D. in Chemical Sciences (Universidad de Castilla-La Mancha (UCLM) and has a master's degree in Biotechnology (Universidad Autónoma de Madrid). Full Professor of Food Microbiology and Food Biotechnology with UCLM. He has spent research periods at the University of California at Davis, Institute of Biotechnology (Stellensbosch. South Africa) and Instituto Agrario Sn Michelle a/Adige (Trento. Italy). He has either conducted or taken part in more than 50 research Regional and National projects and published more than 70 papers in indexed journals or book chapters. He has patented 4 inventions.

Jose Luis Sánchez-Rojas Aldavero received the B.E., M.S., and Ph.D. degrees in telecommunication engineering from the Universidad Politécnica de Madrid, Spain. In 1997, he was an Invited Postdoctoral Scientist with Cornell University, Ithaca, NY, and Colorado University, Boulder. He is currently a Full Professor with the Universidad de Castilla–La Mancha, Ciudad Real, Spain. His research interests cover optical and electrical characterization and modeling of semiconductor devices and MEMS/NEMS sensors.